

萘酰亚胺-卟啉星型电子受体分子的构筑及其在非富勒烯太阳能电池中的应用

周士超^{1,2}, 冯贵涛², 夏冬冬², 李诚^{2,*}, 武永刚^{1,*}, 李韦伟

¹ 河北大学, 化学与环境科学学院, 保定 071002

² 中国科学院化学研究所, 有机固体院重点实验室, 北京 100190

Star-Shaped Electron Acceptor based on Naphthalenediimide-Porphyrin for Non-Fullerene Organic Solar Cells

ZHOU Shichao^{1,2}, FENG Guitao², XIA Dongdong², LI Cheng^{2,*}, WU Yonggang^{1,*}, LI Weiwei^{2,*}

¹ College of Chemistry and Environmental Science, Hebei University, Baoding 071002, Hebei Province, P. R. China.

² CAS Key Laboratory of Organic Solids, Institute of Chemistry, Chinese Academy of Sciences, Beijing 100190, P. R. China.

*Corresponding authors. Email: licheng1987@iccas.ac.cn (LI C); wuyonggang@hbu.edu.cn (WU YG); liweiwei@iccas.ac.cn (LI WW).

Contents

1. Materials and synthesis
2. Solar cells performance
3. AFM and SCLC
4. NMR and MALDI-TOF spectra
5. References

1 Materials and synthesis

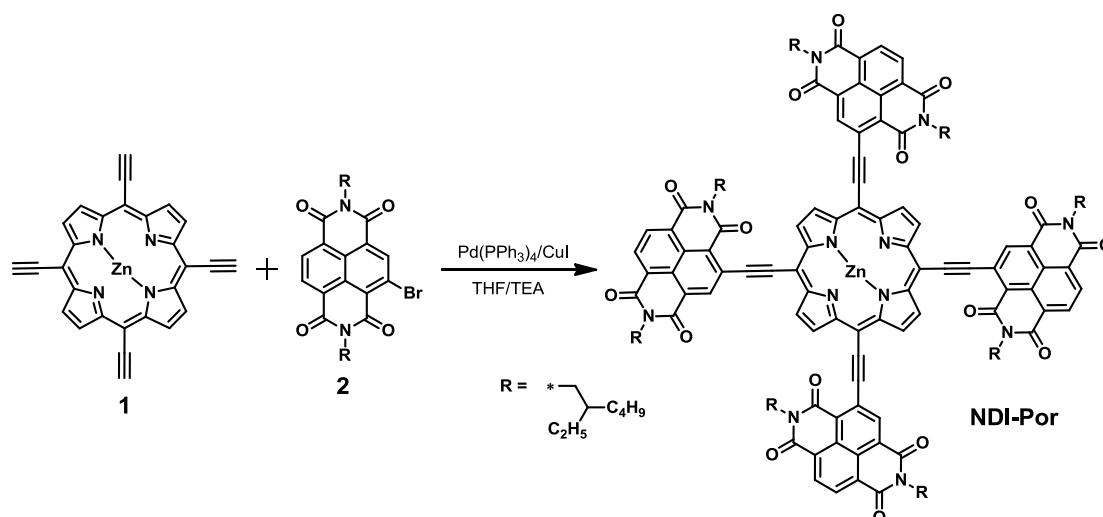
The synthetic procedures were performed under argon atmosphere. Commercial chemicals (from sigma-Aldrich, JK Chemical and TCI) were used as received. Zinc (II) 5,10,15,20-tetraethynylporphyrin (**1**)¹ and 4-bromo-2,7-bis(2-ethylhexyl)benzo[*lmn*] [3,8]phenanthroline-1,3,6,8(2*H*,7*H*)-tetraone (**2**)² were prepared according to literature procedures. Optical absorption spectra were recorded on a JASCO V-570 spectrometer with a slit width of 2.0 nm and a scan speed of 1000 nm min⁻¹. Cyclic voltammetry was performed under an inert atmosphere at a scan rate of 0.1 V·s⁻¹ and 1 mol·L⁻¹ tetrabutylammonium hexafluorophosphate in acetonitrile as the electrolyte, a glassy-carbon working electrode coated with samples, a platinum-wire auxiliary electrode, and an Ag/AgCl as a reference electrode.

Photovoltaic devices with inverted configuration were made by spin-coating a ZnO sol-gel³ at 4000 rpm for 60 s onto pre-cleaned, patterned ITO substrates. The photoactive layer was deposited by spin coating a chlorobenzene solution containing the polymer PBDB-T and the acceptor NDI-Por and the appropriate amount of DIO as processing additive. MoO₃ (10 nm) and Ag (100 nm) were deposited by vacuum evaporation at ca. 7 × 10⁻⁵ Pa as the back electrode.

The active area of the cells was 0.04 cm². The *J*-*V* characteristics were measured by a Keithley 2400 source meter unit under AM1.5G spectrum from a solar simulator (Enlitech model SS-F5-3A). Solar simulator illumination intensity was determined at 100 mW cm⁻² using a monocrystal silicon reference cell with KG5 filter. Short circuit currents under AM1.5G conditions were estimated from the spectral response and convolution with the solar spectrum. The external quantum efficiency was measured by a Solar Cell Spectral Response Measurement System QE-R3011 (Enli Technology Co., Ltd.). The thickness of the active layers in the photovoltaic devices was measured on a Veeco Dektak XT profilometer.

Atomic force microscopy (AFM) images were recorded using a Digital Instruments Nano scope IIIa multimode atomic force microscope in tapping mode under ambient conditions.

The SCLC carrier mobilities were calculated from the slope of the *J*^{1/2}-*V* curves, by fitting the dark current according to the standard trap-free SCLC transport equation: $J = 9\epsilon_0\epsilon_r\mu_h(\mu_e)V^2/8d^3$, where *J* is the measured current density, ϵ_0 is the permittivity of free space, ϵ_r is the relative dielectric constant of the transport material, μ is the mobility, *d* is the thickness of the active layer. *V* is the applied voltage.



Scheme S1 Synthetic procedures for the electron acceptor NDI-Por.

NDI-Por. To a 50 mL two necked round-bottom flask were added **1** (20.06 mg, 0.043 mmol), **2** (121.58 mg, 0.21 mmol), anhydrous THF (5 mL) and triethylamine (1 mL), and the mixture was deoxygenated with argon for 30 min before Pd(PPh₃)₄ (3.00 mg, 0.0026 mmol) and CuI (0.41 mg, 0.0022 mmol) were added. Then the mixture was stirred at 80 °C for 72 h under argon. After cooled to room temperature, the mixture was washed with water and dried over anhydrous Na₂SO₄. Then the solvent was removed,

and the residue was purified by column chromatography on silica gel to give a brown solid **NDI-Por** with yield by 52.9%. MS (HR-MALDI) calc. for $[C_{148}H_{156}N_{12}O_{16}Zn]$: 2424.27; found 2423.1139.

2 Solar cells performance

Table S1 Characteristics of PBDB-T:NDI-Por solar cells spin coated from different ratio of donor to acceptor and additive content.

Ratio	Solvent	Thickness/nm	$J_{sc}/(mA \cdot cm^{-2})$	V_{oc}/V	FF	PCE/%
1:1	CB/DIO (0.5%)	60	5.61	0.63	0.46	1.60
1:1	CB/DIO (1%)	60	6.11	0.63	0.48	1.79
1:1	CB/DIO (1.5%)	60	6.05	0.65	0.46	1.80
1:1	CB/DIO (2.5%)	55	5.69	0.63	0.45	1.62
2:1	CB/DIO (1.5%)	70	4.57	0.63	0.41	1.19
1:2	CB/DIO (1.5%)	70	4.24	0.63	0.42	1.12

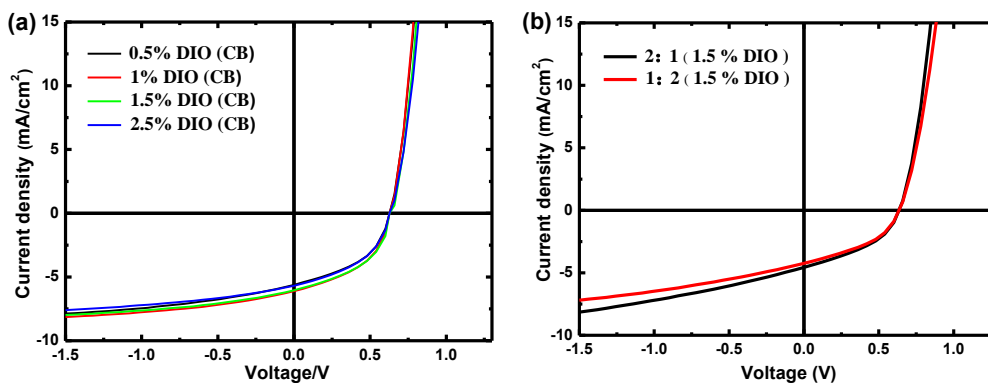


Fig.S1 J-V characteristics of the J-V characteristics in the dark (dashed line) and under illumination with white light.

3 AFM and SCLC

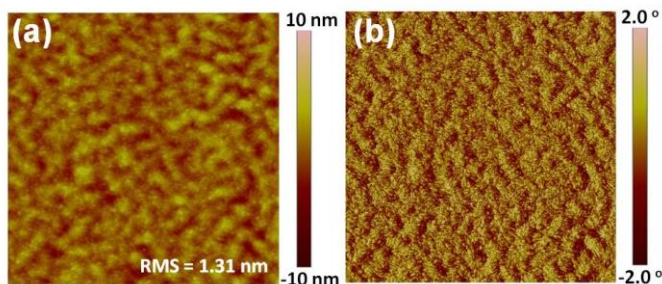


Fig S2 (a) AFM height image ($3 \mu m \times 3 \mu m$) of optimized PBDB-T:PBI-Por thin film spin-coated from CB with 1% DIO. (b) The corresponding phase image.

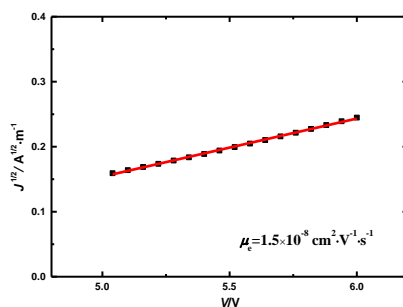


Fig.S3 J-V characteristics of PBI-Por electron-only devices under dark spin-coated from CB with 1% DIO.

4 NMR and MALDI-TOF spectra

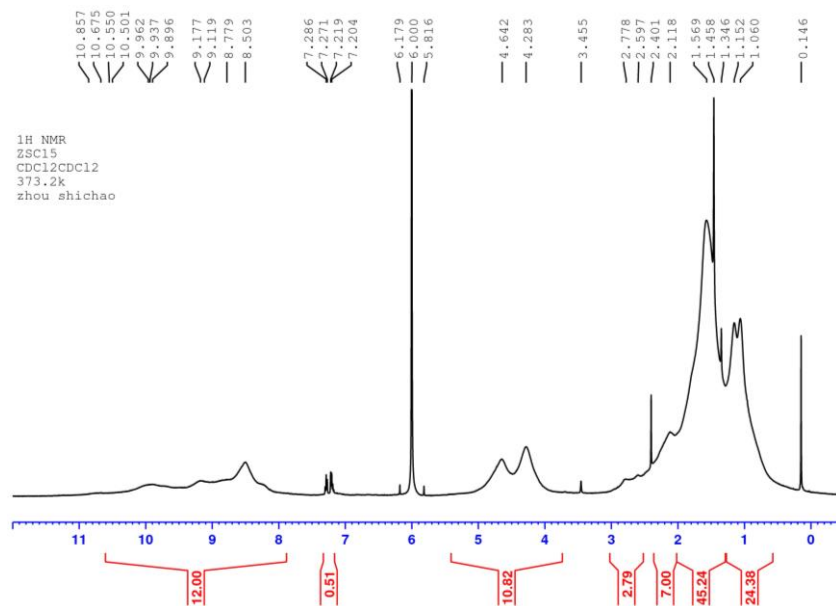


Fig.S4 ¹H-NMR of NDI-Por recorded at 100 °C with 1,1,2,2-tetrachloroethane-d₄ as the solvent.

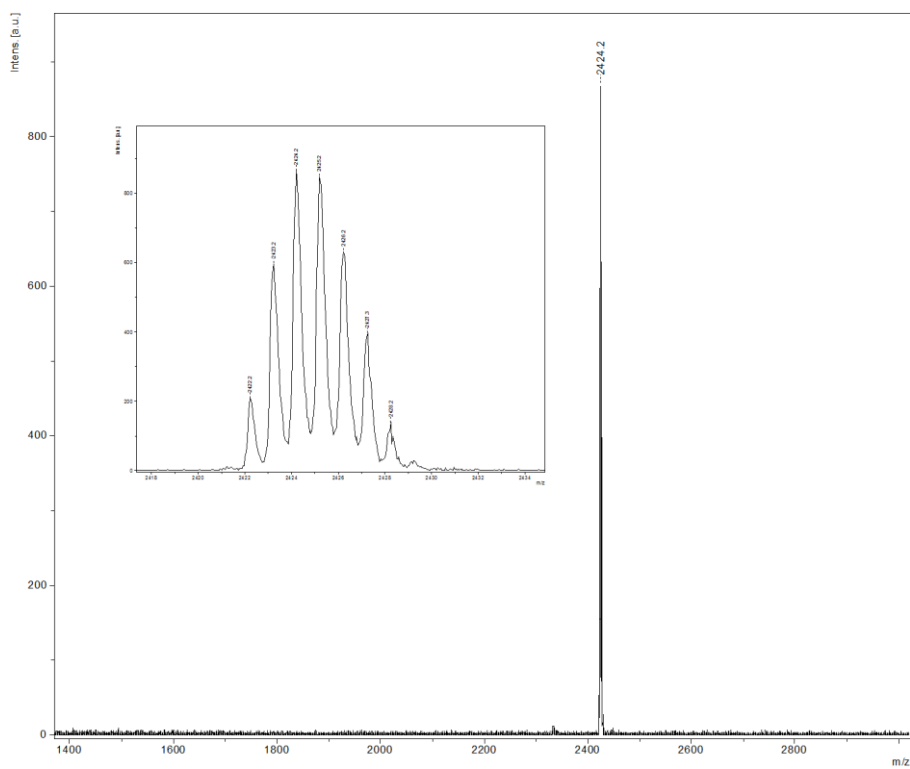


Fig.S5 MALDI-TOF of NDI-Por.

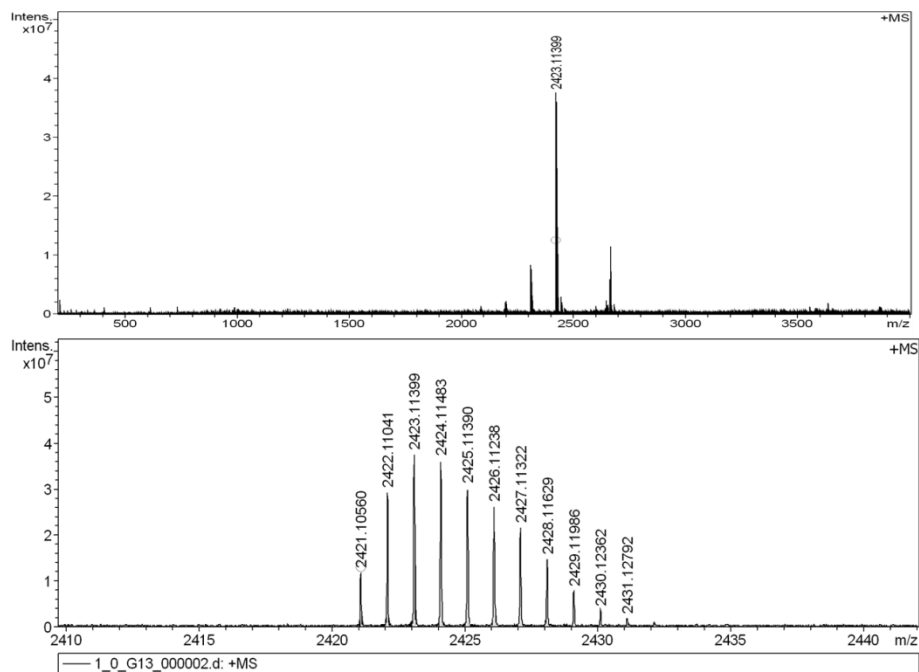


Fig.S6 High resolution MALDI-TOF of NDI-Por.

5 References

- (1) Yen, W. N.; Lo, S. S.; Kuo, M. C.; Mai, C. L.; Lee, G. H.; Peng, S.-M.; Yeh, C. Y. *Org. Lett.* **2006**, *8*, 4239. doi:10.1021/ol061478w.
- (2) Liu, Y.; Zhang, L.; Lee, H.; Wang, H.-W.; Santala, A.; Liu, F.; Diao, Y.; Briseno, A. L.; Russell, T. P. *Adv. Energy Mater.* **2015**, *5*, 1500195. doi:10.1002/aenm.201500195.
- (3) Sun, Y. M.; Seo, J. H.; Takacs, C. J.; Seifert, J.; Heeger, A. J. *Adv. Mater.* **2011**, *23*, 1679. doi:10.1002/adma.201004301.